TRANSONIC FLIGHT FLUTTER TESTS OF A CONTROL SURFACE UTILIZING AN IMPEDANCE RESPONSE TECHNIQUE

L. I. Mirowitz —McDonnell Aircraft Corporation,
St. Louis, Missouri

- -

Abstract

Transonic flight flutter tests of the XF3H-1 "Demon" Airplane have been conducted utilizing a frequency response technique in which the oscillating rudder provides the means of system excitation. These tests were conducted as a result of a rudder flutter incident in the transonic speed range. The technique employed is presented including a brief theoretical development of basic concepts. Test data obtained during the flight are included and the method of interpretation of these data is indicated. This method is based on an impedance matching technique. It is shown that an artificial stabilizing device, such as a damper, may be incorporated in the system for test purposes without complicating the interpretation of the test results of the normal configuration. Data are presented which define the margin of stability introduced to the originally unstable rudder by design changes which involve higher control system stiffness and external damper. It is concluded that this technique of flight flutter testing is a feasible means of obtaining flutter stability information in flight.

INTRODUCTION

With the initiation of the first flight of the XF3H-1 Airplane — the prototype version of the F3H-1 "Demon", Figure 1 — a flight flutter test program was conducted concurrently with the speed build-up of the airplane. This program consisted of the transient response technique of flight flutter testing through pilot induced control surface impulse motion. However, during the course of this flight flutter test program, a neutrally stable empennage flutter condition was encountered at a Mach number of 1.04 and an altitude of about 30,000 feet. Records taken during the flight indicated that the flutter condition emanated from the fin-rudder system with a frequency of 20 cycles per second. As a result of this, a program was initiated consisting of theoretical investigations in conjunction with flight flutter testing in order to establish the cause of the instability and to guide in the determination of corrective measures.

This paper concerns itself with the concepts and results obtained from the subsequent flight flutter test program. The theoretical concepts underlying the approach which was utilized, and which involves in particular a frequency response technique in which the oscillating rudder is utilized as the aeroelastic forcing system, have been presented in R. A. Pepping's paper, "A Theoretical Investigation of the Oscillating Control Surface Frequency Response Technique of
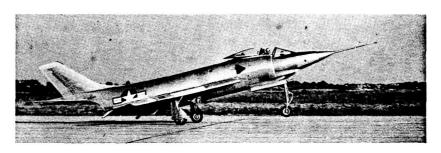

Figure 1.

Flight Flutter Testing", Journal of the Aeronautical Sciences, August 1954, Volume 21, No. 8. The idea behind this approach involves the concept of impedance matching as applied to dynamic aeroelastic systems. For convenience, a summary of the theoretical development is repeated herein.

THEORETICAL BACKGROUND

In order to determine the flutter stability of a system which has incorporated a servo control mechanism, it is important that the dynamic behavior of the servo be included in the flutter investigation in combination with the structural, inertia, and aerodynamic contribution of the remaining control surface-primary surface system. In addition to acting as a control surface restraint mechanism, the servo serves also as a control actuation system which receives its signal either from the pilot, a radar beam, or from a sensing element in the fuselage in which case it becomes part of the autopilot system of the airplane. A method showing the interaction of the servo-control surface-airplane system is the block diagram representation used frequently in the theory of servo mechanism analysis which schematically traces through the events which take place when a signal is received by the servo resulting in motion of the airplane from its predetermined or pilot-set path.

Block Diagram Representation of the Aeroelastic System

The system analyzed consists of the control surface-airplane flutter system, the servo system, and the return loop from the airplane fuselage sensing element (gyro) back to the servo. In block diagram form, this feed-back system may be represented as shown in Figure 2. The impedance of the aeroelastic

system and the control system is defined as the moment applied to each system per unit deflection to sustain motion at any given frequency. As seen from the block diagram, the complete system consists of two feed-back loops. Loop 1, the inner loop, accounts for the fact that the servo — which could be, for example, a hydraulic actuator — acts as a root restraint for the control surface, tending to return the control surface to neutral upon deflection. Loop 2, the outer loop, accounts for the servo as part of the autopilot system, sensing airplane motion away from the set path with resultant corrective action.

In this paper we will confine ourselves of the dynamic character of the inner loop, or Loop 1, since the autopilot of the airplane is not of immediate interest. The block diagram for the inner loop, Loop 1, is again shown in Figure 3 where Z_β is the impedance of the servo mechanism, i.e., the hydraulic actuator, obtained from calculations or from measured frequency response data, and where M_β is the moment
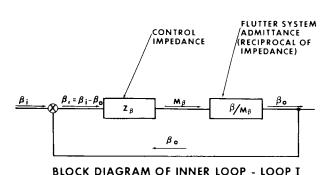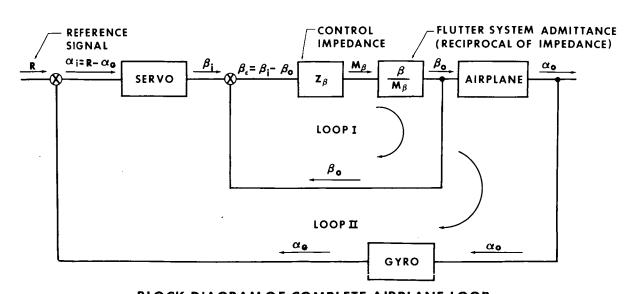

BLOCK DIAGRAM OF INNER LOOP - LOOP I

Figure 3.

BLOCK DIAGRAM OF COMPLETE AIRPLANE LOOP

Figure 2.

required to deflect the control surface through an angle β measured at the point of moment application. This can be measured in flight or can be idealized mathematically by a number of degrees of freedom such as surface torsion, surface bending, fuselage bending, and control surface rotation. The equations of motion for the inner loop are given in Figure 4 in terms of the ratio of output over input. From the equations of motion the characteristic equation defining the frequency parameters of the system and its stability is given by the denominator of equation 1.0 as equation 1.1. Neutral stability is determined if there exists a finite frequency which satisfies equation 1.1 or, as stated in 1.2, there exists a hinge moment impedance at some finite frequency which is equal and opposite to the control system impedance.

EQUATION OF MOTION:

$$\frac{OUTPUT}{INPUT} = \frac{\beta_o}{\beta_i} = \frac{Z_\beta \left(\dfrac{\beta}{M_\beta}\right)}{Z_\beta \left(\dfrac{\beta}{M_\beta}\right) + 1} = \frac{1}{1 + \left(\dfrac{M_\beta}{\beta}\right)\dfrac{1}{Z_\beta}} \qquad 1.0$$

CHARACTERISTIC EQUATION:

$$1 + \left(\frac{M_\beta}{\beta}\right)\frac{1}{Z_\beta} = 0 \qquad 1.1$$

NEUTRAL STABILITY CRITERION:

$$\left(\frac{M_\beta}{\beta}\right)\frac{1}{Z_\beta} = -1 \qquad (a)$$

$$\left(\frac{M_\beta}{\beta}\right) = -Z_\beta \qquad (b)$$

$$\left.\begin{array}{c} \\ \\ \end{array}\right\} \quad 1.2$$

BASIC STABILITY CRITERIA

Figure 4.

Idealization of Aeroelastic Impedance

From the theoretical standpoint the aeroelastic impedance of the control surface can be idealized schematically by the three-degrees-of-freedom: primary surface bending, primary surface torsion, and control surface rotation as shown in Figure 5. This idealization is the minimum required to cover all the concepts of the approach utilized herein — additional degrees of freedom may be added as necessary without invalidating any of these concepts. The upper diagram is the idealization of the flutter system. The lower diagram is the idealization of the control system. The equations of motion of the flutter system as actuated by the driving hinge moment M_β is shown in Figure 6, equation 2.1. Solving from 2.1 for the impedance M_β / β , equation 2.2 is obtained. As seen, the rudder hinge moment impedance is the ratio of two stability determinants: the numerator is the stability determinant of the aeroelastic flutter
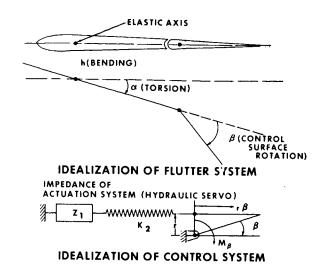

IDEALIZATION OF FLUTTER SYSTEM

IMPEDANCE OF ACTUATION SYSTEM (HYDRAULIC SERVO)

IDEALIZATION OF CONTROL SYSTEM

Figure 5.

$$M_\beta = \left(E_{\beta\beta}\right)_o \beta + E_{\beta h}\cdot H + E_{\beta\alpha}\cdot\alpha$$
$$O = E_{h\beta}\cdot\beta + E_{hh}\cdot H + E_{h\alpha}\cdot\alpha$$
$$O = E_{\alpha\beta}\cdot\beta + E_{\alpha h}\cdot H + E_{\alpha\alpha}\cdot\alpha$$

Where:
$$E_{jk} = R_{jk} + iI_{jk} - \sigma_{ojk} \qquad \text{for } j \neq k$$
$$E_{ii} = R_{ii} + iI_{ii} - \sigma_{oii}\left[1 - \frac{\omega_{ii}^2}{\omega^2}\left(1 + ig_{ii}\right)\right]$$
$$\left(E_{ii}\right) = E_{ii} - \sigma_{oii}\frac{\omega_{ii}^2}{\omega^2}\left(1 + ig_{ii}\right) = E_{ii} - Z_i$$

$$\qquad 2.1$$

From 2.1

$$\frac{M_\beta}{\beta} = \frac{D_o}{N_{\beta\beta}} = \frac{f(\omega)}{g(\omega)} = \frac{\pi_\rho b_o^4 \omega^2 \begin{vmatrix} \left(E_{\beta\beta}\right)_o & E_{\beta h} & E_{\beta\alpha} \\ E_{h\beta} & E_{hh} & E_{h\alpha} \\ E_{\alpha\beta} & E_{\alpha h} & E_{\alpha\alpha} \end{vmatrix}}{\begin{vmatrix} E_{hh} & E_{h\alpha} \\ E_{\alpha h} & E_{\alpha\alpha} \end{vmatrix}} \qquad 2.2$$

ANALYTICAL EXPRESSION FOR IMPEDANCE - M_β / β

Figure 6.

system with free-floating or unrestrained control surface and the denominator is the flutter stability determinant for infinite restraint in rotation or, in other words, rotation is not a degree of freedom. The stability determinant for the denominator would be the primary surface flutter stability determinant.

Stability Criterion

Figure 7 again shows the characteristic equation of the inner loop as equation 3.1. Substituting equation 2.2 into equation 3.1, the characteristic equation is rewritten as equation 3.2 in terms of the stability determinants of the aeroelastic flutter sys-

CHARACTERISTIC EQUATION :

$$Z_\beta + \frac{M_\beta}{\beta} = 0 \qquad\qquad 3.1$$

FROM 2.2:

$$\frac{M_\beta}{\beta} = \frac{D_o}{N_{\beta\beta}} \qquad\qquad (a)$$

$$Z_\beta + \frac{M_\beta}{\beta} = \frac{D_o + Z_\beta\ N_{\beta\beta}}{N_{\beta\beta}} \qquad (b) \qquad\qquad 3.2$$

FROM 2.1:

$$D_o + Z_\beta N_{\beta\beta} = D = \text{STABILITY DETERMINANT WITH CONTROL}$$
$$\text{SURFACE RESTRAINED BY } Z_\beta \qquad\qquad 3.3$$

FROM 3.3 AND 3.2(b):

$$Z_\beta + \frac{M_\beta}{\beta} = \frac{D}{N_{\beta\beta}} \qquad\qquad 3.4$$

3.4 STATES THAT BOTH $\left(Z_\beta + \frac{M_\beta}{\beta}\right)$ AND D DEFINE THE STABILITY OF THE
FLUTTER SYSTEM WITH THE CONTROL SURFACE RESTRAINED BY
Z_β, THUS THE STABILITY IS RELATED TO THE MEASURABLE
DRIVING HINGE MOMENT.

STABILITY EQUATIONS

Figure 7.

tem. The numerator of 3.2 is the stability determin-ant with the control surface restrained by the control system impedance, Z_β. This determinant is denoted as D. Substituting 3.3 into 3.2, the characteristic equation 3.1 is transformed into 3.4 which states that both $(Z_\beta + M_\beta/\beta)$ and D define the stability of the flutter system with a control surface restrained by Z_β. Thus the stability is related to the measurable driving hinge moment. The characteristic equation 3.4 will determine the system stability. In general, the numerator of the right hand side of 3.4, D, is a differential equation of rth order and the denominator $N_{\beta\beta}$ is a differential equation of nth order. The problem then, is to determine if there exist any roots of the numerator which are characterized by a posi-tive exponential decay function (divergence) which would indicate instability or by a zero decay function which would indicate neutral stability. If the equa-tions are written in differential equation form, then the roots of the stability equation or of the stability determinant, D, may be solved for directly. This is roughly the case of theoretical flutter analysis. How-ever, equation 3.4 states that stability may also be determined as a measure of the driving hinge mo-ment impedance, M_β/β, for this is a measurable quantity.

In the theory of servo mechanisms, a relation-ship is drawn between the determination of system stability from the solution of the differential equa-tions (transient stability) and the results from the frequency response behavior of the dynamic system. The frequency response technique is denoted as the Nyquist approach. In this case the differential equa-tions of motion are written in transformed form and the system is analyzed without solving for the roots by an examination of the behavior of the response $(M_\beta/\beta + Z_\beta)$ as the frequency is varied from minus

infinity to plus infinity. For stability, none of the roots of the transformed characteristic equation — the numerator of 3.4 - may have a positive real part.

By the use of a modified Nyquist approach, this is established by observing the behavior of the re-sponse vector $(M_\beta/\beta + Z_\beta)$ as the frequency is varied from minus infinity to plus infinity. If there are any roots with positive real part — which denotes instability — the vector $(M_\beta/\beta + Z_\beta)$ will perform as many clockwise rotations about the origin when plotted on a complex plane as there are roots with positive real parts. It is possible, however, also to have roots in the denominator of the vector equation 3.4 with positive real parts. Roots in the denominator $N_{\beta\beta}$, are denoted as poles and are the solutions of the flutter system with infinite restraint in the control system. In that case, the vector equation 3.4 will perform as many counterclockwise rotations about the origin as there are poles with positive real parts. Since both conditions can exist simultaneously, then for the system to be stable — or no unstable roots in the numerator of 3.4 — the direction of rotation of the vector $(M_\beta/\beta + Z_\beta)$ about the origin must be counterclockwise and the number of rotations must be equal to the number of unstable poles.

If there are no unstable poles, or in other words, there are no unstable roots in the denominator, and therefore, the primary surface is flutter-free with an infinitely restrained control surface, then for the system to be stable, the vector $(M_\beta/\beta + Z_\beta)$ must not envelop or rotate about the origin. In this latter case, simple energy concepts will also lead to the same conclusions regarding the definition of stability, for example, Pepping's paper referred to previously discusses the energy approach.

Figure 8 presents the ground rules for applying the modified Nyquist stability criterion to the imped-ance stability plots. It should be noted that in actual practice the frequency variation can be limited to a reasonable range enveloping the suspected flutter frequency. Figure 9 indicates a particular application of the impedance plots and shows a speed which would be unstable and a neutrally stable speed and relates this to the well known flutter stability plot of velocity versus control surface rotational frequency.
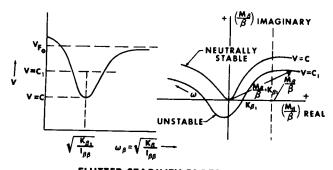
Quite often instead of utilizing the complex plane plots of the impedance vector an alternate method is applied which makes use of the so-called phase margin plot. This is shown in Figure 10.

The significance of the impedance matching ap-proach is as follows. The aeroelastic impedance, M_ρ/β may be calculated or measured. It is then a given known quantity for a given set of conditions independent of the restraint, Z_β. The restraining impedance, Z_β, may be measured or calculated. The

MODIFIED NYQUIST STABILITY CRITERION:

1. For each forward velocity and a reasonable frequency range, measure or calculate M_β/β vs. ω.

2. Add to M_β/β the measured or calculated control system impedance Z_β and obtain $M_\beta/\beta + Z_\beta$ vs. ω. Plot on a complex plane for each forward velocity.

3. Calculate the flutter speed or speeds of the system with infinite control surface restraint. This is designated as V_{F_0}.

4. For velocities less than V_{F_0} the system is <u>stable</u> if the vector $M_\beta/\beta + Z_\beta$ <u>does not</u> envelop the origin.

5. For velocities greater than V_{F_0} the system is <u>stable only</u> if the number of counterclockwise rotations about the origin of $M_\beta/\beta + Z_\beta$ is equal to the number of V_{F_0}'s.

6. For any velocity the system is <u>neutrally stable</u> if $M_\beta/\beta + Z_\beta$ passes through the origin.

Figure 8.

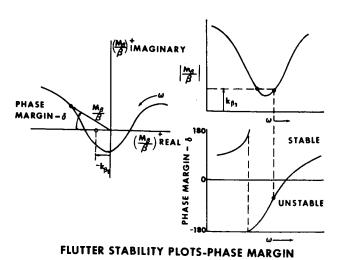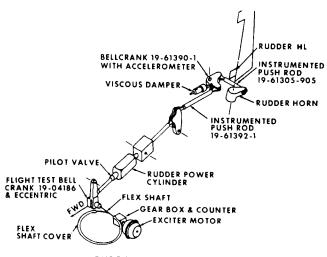

FLUTTER STABILITY PLOTS-IMPEDANCE

Figure 9.

FLUTTER STABILITY PLOTS-PHASE MARGIN

Figure 10.

vector sum of the two determines the stability of the total system. Additional devices which modify the restraining impedance Z_β, may be evaluated without further experimental work in flight once the aeroelastic impedance, M_β/β has been established uniquely.

TEST CONFIGURATION

The flutter testing of the XF3H-1 rudder is based on the theory presented in the previous discussion. The hinge moment M_β was supplied by the hydraulic actuating cylinder through sinusoidal operation of the actuator valve. This is shown in Figure 11 which presents a schematic of the shaker system.
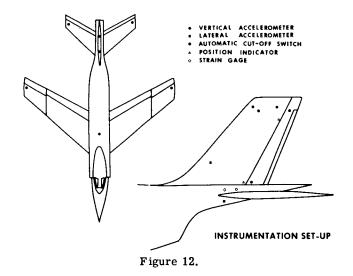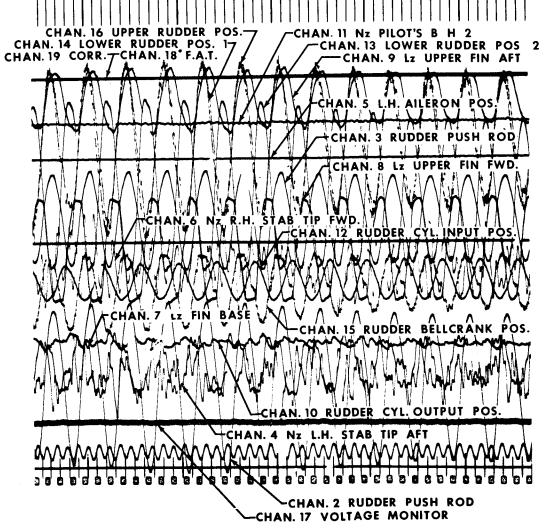

RUDDER EXCITER INSTALLATION

Figure 11.

Also added to the system was a viscous damper for stability reasons. Figure 12 indicates the type of instrumentation employed on the airplane for these tests. One of the strain gages shown in this figure was installed on the control rod leading directly into the rudder and gave a definition of the driving hinge moment, M_β, and the other was installed on the control rod just upstream from the damper to define the hinge moment of the rudder as restrained by the damper. The damper was a non-linear velocity squared damping device.

TEST PROCEDURE

The general technique of testing consisted of stabilizing the airplane at a constant Mach number at about 30,000 feet altitude (this was the altitude at which all the test data was obtained) and varying the fre-

- VERTICAL ACCELEROMETER
- LATERAL ACCELEROMETER
- AUTOMATIC CUT-OFF SWITCH
- POSITION INDICATOR
- STRAIN GAGE

INSTRUMENTATION SET-UP

Figure 12.

CHAN. 16 UPPER RUDDER POS.
CHAN. 14 LOWER RUDDER POS. 1
CHAN. 19 CORR.—CHAN. 18° F.A.T.
CHAN. 11 Nz PILOT'S B H 2
CHAN. 13 LOWER RUDDER POS 2
CHAN. 9 Lz UPPER FIN AFT
CHAN. 5 L.H. AILERON POS.
CHAN. 3 RUDDER PUSH ROD
CHAN. 8 Lz UPPER FIN FWD.
CHAN. 6 Nz R.H. STAB TIP FWD.
CHAN. 12 RUDDER CYL. INPUT POS.
CHAN. 7 Lz FIN BASE
CHAN. 15 RUDDER BELLCRANK POS.
CHAN. 10 RUDDER CYL. OUTPUT POS.
CHAN. 4 Nz L.H. STAB TIP AFT
CHAN. 2 RUDDER PUSH ROD
CHAN. 17 VOLTAGE MONITOR

TYPICAL OSCILLOGRAPH TRACE

Figure 13.

quency of oscillation through the range of about 5 through 35 cps. This range was chosen as being sufficient to envelop the flutter frequency previously encountered.

Oscillations were introduced through hydraulic actuator displacement of the rudder through suitable valve motion. The rudder driving hinge moment upstream and downstream of the damper was measured as well as the rudder angular deflection. This procedure was repeated at successively higher values of Mach number to establish the trend of stability with increasing Mach number.

Rudder static deflections of approximately a degree and a half were employed. The frequency variation was accomplished by an automatically operating rotary switch located in the cockpit and approximately 3 seconds were devoted to each frequency point. Sufficient fatigue strength was provided in the power cylinder back-up structure and in the connecting links so that these components were good for 50,000 cycles of rudder limit hinge moment. Strategically located acceleration sensing devices were tied into the circuitry of the drive motor which were set to turn off the drive motor whenever excess accelerations were encountered. Dynamic measurements throughout the airplane were taken during these tests and the data were recorded on the airplane oscillograph.

TEST RESULTS

A typical oscillograph trace is shown in Figure 13. The instrumentation was somewhat primitive by present day standards; however, the test was conducted in 1952 and much of the more sophisticated types of recording transducers and data reduction machines were not available at that time. Several problems which were encountered with this instrumentation were:

(1) Rudder angles of about a quarter of a degree or less were difficult to measure and some drift in the measurements occurred. Continuous calibration of the position indicators was required in order to hold down the errors from this source

(2) Accelerometers in the tail assembly were not temperature compensated and no accurate definition of the characteristics of the tail oscillations could be obtained. Temperature measurements were recorded for several locations in the tail assembly and this data was used to correct the measured test results

(3) Power cylinder valve displacement and power cylinder output displacement could not be obtained correctly.
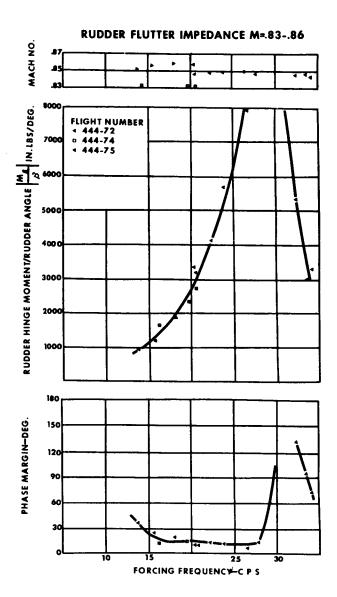

Figure 14.

The data shown in Figure 13 were manually reduced and typical plots for various Mach numbers of the test results are shown in Figures 14 and 16 through 18. The plots cover the Mach number range of .85 to 1.16 and are representative of the impedance data taken through M = 1.26 for the system with and without damper. Data for each Mach number plot were obtained during several flights as indicated. Positive phase margins indicate stability. Negative phase margins indicate instability. To determine the stability of the actual restrained rudder, this data must be combined with the control system impedance, $|Z_\beta|$. Stability is determined by the phase margin existing when $|H_\beta/\beta|$ is equal to $|Z_\beta|$. The hinge moment data obtained at M = 1.04 were utilized in a

RUDDER FLUTTER IMPEDANCE M=1.04

FLIGHT NO.
- ▼ 444-88
- ▶ 444-93
- ◢ 444-94
- ◣ 444-95
- ▲ 444-98
- ▼ 444-100
- ◀ 444-101

Figure 15.

As noted, this data does not indicate a zero phase margin point at M = 1.04 which was the Mach number of the flutter experienced during the initial stages of the flight flutter testing of the airplane. However, the frequency of flutter is correlated.

Tests of the hydraulic actuator impedance indicated that in this frequency range the system was not acting as a pure spring but that some negative phase margin was contributed by the actual impedance of the hydraulic power cylinder. A measure of this loss in phase margin is indicated as the shaded area around M = 1.04. An increase in control system stiffness to 1740 in. lbs per degree which was basically obtained by a more powerful power cylinder is shown by the dashed curve. This increase in stiffness increases the stability of the rudder around M = 1.04; however, it also indicates that the second unstable

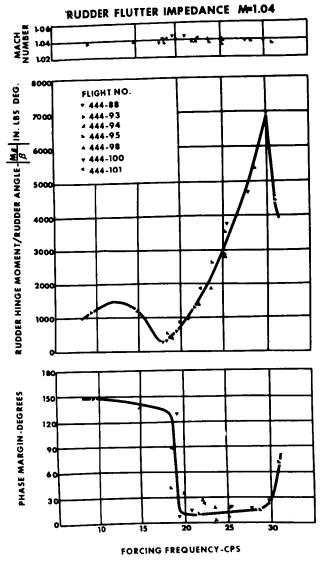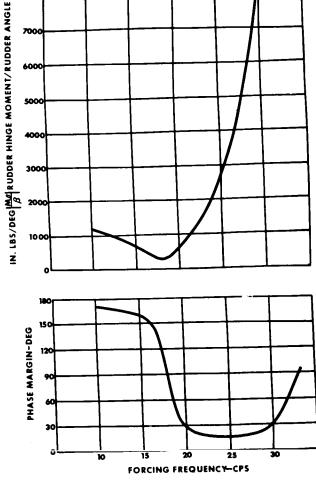## COMPUTED RUDDER FLUTTER IMPEDANCE BASED ON TEST RESULTS AT M=1.04

Figure 16.

theoretical study in order to determine which of the possible critical degrees of freedom of the aeroelastic system are influential in the flutter system. It was found that utilization of the two degrees of freedom, rudder rotation, and rudder torsion, was sufficient to describe reasonably well the variation of the hinge moment and phase margin with frequency at this Mach number. This is shown in Figure 15.

The measured test results have been plotted for two restraint conditions of the rudder; one, the restraint of the original control system – 880 in. lb/degree, and the other, that of the final control system – 1740 in. lb/degree. This is shown in Figure 19, for the idealization of the impedance of the control system as a pure spring without hydraulic damper.
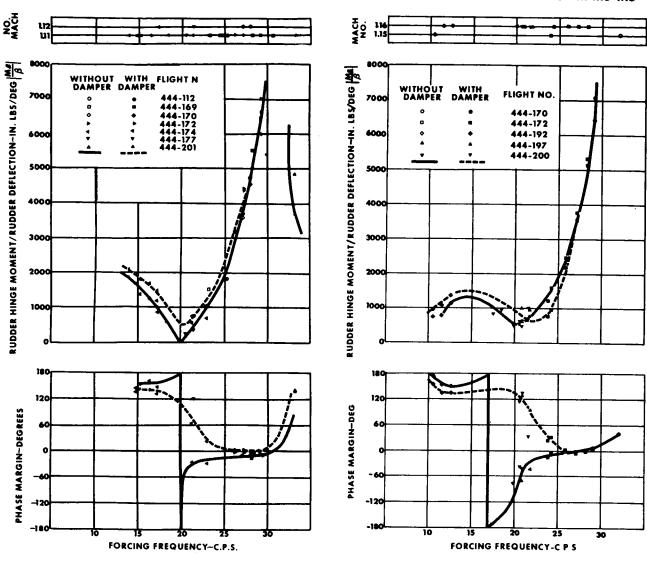
150

Figure 17.

Figure 18.

Mach number range around M = 1.1 is not stabilized markedly by this stiffness change even though some improvement in phase margin is indicated. From this data, it was concluded that stiffness alone will not eliminate the flutter instability on the rudder. The stability of the system with the damper and the stiffer control system (final configuration) is indicated in Figure 20. An additional gain in phase margin is shown with adequate stability existing throughout the applicable Mach number range. Similar plots were constructed for various combinations of damper and power cylinder impedance characteristics.
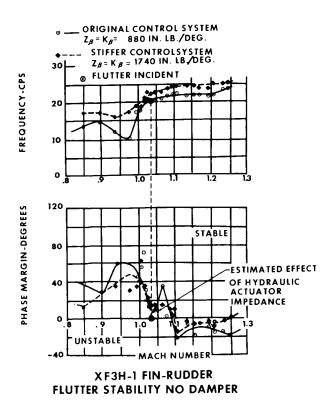
ORIGINAL CONTROL SYSTEM
$Z_\beta = K_\beta =$ 880 IN. LB./DEG.

STIFFER CONTROL SYSTEM
$Z_\beta = K_\beta =$ 1740 IN. LB./DEG.

⊗ FLUTTER INCIDENT

STIFFER CONTROL SYSTEM
$Z_\beta = K_\beta =$ 1740 IN. LB./DEG.
WITH DAMPER

XF3H-1 FIN-RUDDER
FLUTTER STABILITY NO DAMPER

Figure 19.

XF3H-1 FIN-RUDDER
FLUTTER STABILITY
WITH DAMPER

Figure 20.

CONCLUSIONS

On the basis of this discussion, the following is concluded:

(1) The impedance matching technique of determining stability is a feasible means of conducting flight flutter testing.

(2) The interpretation of the test data is straightforward and revolves mainly around the determination of the aeroelastic impedance vector of an oscillating control surface.

(3) The aeroelastic impedance can be determined in flight utilizing a control surface which has been stabilized artificially and information from this data may be obtained for a variety of artificial stabilization systems. These stabilization systems may take the form of external dampers or stabilizing feed-back signals.
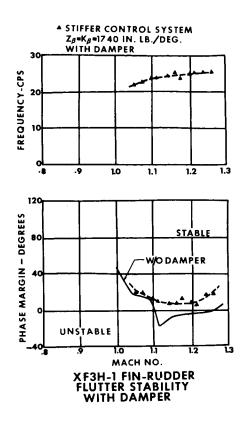
REFERENCES

1. Pepping, R. A., A Theoretical Investigation of the Oscillating Control Surface Frequency Response Technique of Flight Flutter Testing, Journal of the Aeronautical Sciences, Vol. 21, No. 8, August 1954.

2. Chestnut, Harold and Mayer, Robert W., Servomechanisms and Regulating System Design, Vol. 1, John Wiley and Sons, Inc., New York, 1951.

3. Mirowitz, L. I., Flutter Stability of a Wing with Servo Root Restraint and Automatic Servo Control, McDonnell Aircraft Corporation Internal Engineering Note, 1 July 1953.

4. Mirowitz, L. I., F3H-1 Airplane, Flutter Analysis Summary Report, McDonnel Aircraft Corporation Engineering Report No. 3333, 23 December 1953.

SYMBOLS

M_β = oscillatory rudder hinge moment.

β = rudder deflection.

M_β/β = flutter impedance of the rudder aeroelastic system.

Z_β = rudder control system impedance.

$\left.\begin{array}{l} R_{jk} + \\ iI_{jk} \end{array}\right\}$ = oscillatory flow aerodynamic derivative.

$\left.\sigma_{o_{jk}}\right.$ = inertia derivative.

$\left.\omega_{jj}\right.$ = natural frequency of a degree of freedom in equations of motion.

$\left.\begin{array}{c}\\ \\ \end{array}\right\}$ See Equation 2.1

ω = circular frequency.

ρ = air density.

b_o = reference semichord.

δ = phase margin — 180° less the phase angle.

Subscripts:

o = output.

i = input.

ϵ = error or input less output.